New Phytologist

Reduced gibberellin response affects ethylene biosynthesis and responsiveness in the Arabidopsis *gai eto2-1* double mutant

Liesbeth De Grauwe[1], Laury Chaerle[1], Jasper Dugardeyn[1], Jan Decat[1], Ivo Rieu[2], Wim H. Vriezen[1], Thomas Moritz[3], Gerrit T. S. Beemster[4], Andy L. Phillips[2], Nicholas P. Harberd[5], Peter Hedden[2] and Dominique Van Der Straeten[1]

[1]Unit Plant Hormone Signaling and Bio-Imaging, Department of Molecular Genetics, Ghent University, K.L. Ledeganckstraat 35, B-9000 Gent, Belgium; [2]Crop Performance Improvement Division, Rothamsted Research, Harpenden AL5 2JQ, Herts, UK; [3]Umeå Plant Science Centre, Department of Forest Genetics and Plant Physiology, Swedish University of Agricultural Sciences, SE-901 87 Umeå, Sweden; [4]Plant Systems Biology, Flemish Institute of Biology (VIB)/Ghent University, Technologiepark 927, B-9052 Gent, Belgium; [5]John Innes Centre, Norwich NR4 7UJ, UK

Author for correspondence:
Dominique Van Der Straeten
Tel: +32 9264 5185
Fax: +32 9264 5333
Email: Dominique.VanDerStraeten@ugent.be

Received: *7 August 2007*
Accepted: *12 August 2007*

Summary

• Ethylene and gibberellins (GAs) control similar developmental processes in plants. The role of ethylene is at least in part to regulate the accumulation of DELLA proteins, key regulators of plant growth, which suppress the GA response.

• To expand our knowledge of ethylene–GA crosstalk and to reveal how the modulation of the ethylene and GA pathways affects global plant growth, the gibberellin-insensitive (*gai*), ethylene-overproducing 2-1 (*eto2-1*) double mutant, which has decreased GA signalling (resulting from *gai*) and increased ethylene biosynthesis (resulting from *eto2-1*), was characterized.

• Both single mutations resulted in reduced elongation growth. The double mutant showed synergistic responses in root and shoot growth, in induction of floral transition, and in inflorescence length, showing that crosstalk between the two pathways occurs in different plant organs throughout development. Furthermore, the altered ethylene–GA interactions affected root–shoot communication, as evidenced by an enhanced shoot:root ratio in the double mutant. When compared with both single mutants and the wild type, double mutants had enhanced content of active GA_4 at both the seedling and the rosette stages, and, unlike the *gai* mutant, they were sensitive to GA treatment.

• Finally, it was shown that synergistic responses in the double mutant were not caused by elevated ethylene biosynthesis but that, in the light, enhanced sensitivity to ethylene may, at least in part, be responsible for the observed phenotype.

Key words: Arabidopsis, crosstalk, ethylene, gibberellins, growth, root:shoot ratio.

New Phytologist (2008) **177**: 128–141

doi: 10.1111/j.1469-8137.2007.02263.x

Introduction

Interactions between hormones have been demonstrated for several plant developmental stages, from hypocotyl elongation and the formation of the apical hook to the determination of leaf and shoot form, tropic and nastic movements of the shoot, and the control of flowering (Vandenbussche & Van Der Straeten, 2004; Achard *et al.*, 2006, 2007). Crosstalk between gibberellins (GAs) and ethylene, as well as with other hormones such as auxins, has been demonstrated (Achard *et al.*, 2003; Fu & Harberd, 2003; Vriezen *et al.*, 2004; De Grauwe *et al.*, 2007). DELLA proteins, which act as nuclear repressors of

GA signalling, appear to be key integrators in the GA–ethylene crosstalk. They are members of the GRAS family of transcriptional regulators – gibberellin insensitive (GAI), repressor of *ga1-3* (RGA), and SCARECROW – which are characterized by the conserved N-terminal (DELLA) domain (Richards *et al.*, 2001). In Arabidopsis, the DELLA family comprises GAI, RGA and RGA-like 1/2/3 (RGL1/2/3) (Peng *et al.*, 1997; Silverstone *et al.*, 1998, 2001; Lee *et al.*, 2002; Wen & Chang, 2002). These proteins are rapidly destabilized after GA treatment through degradation by the 26S proteasome (Silverstone *et al.*, 1998; Dill & Sun, 2001; Fu *et al.*, 2002). The destabilization is an effect of polyubiquitination and subsequent degradation by means of the ubiquitin proteasome system involving the Skp1/cullin/F-box (SCF) E3 ubiquitin ligase enzyme complex. In Arabidopsis, DELLA proteins are targeted for degradation by the F-box protein Sleepy 1 (SLY1) (McGinnis *et al.*, 2003; Dill *et al.*, 2004; Fu *et al.*, 2004), binding to which is enhanced by interaction with the soluble GA receptors gibberellin-insensitive dwarf 1a/b/c (AtGID1a/b/c) in the presence of GA (Griffiths *et al.*, 2006; Nakajima *et al.*, 2006). The N-terminal DELLA domain is required for binding of the DELLA proteins to the GA–GID1 complex (Griffiths *et al.*, 2006).

Ethylene has been shown to delay the disappearance of a green fluorescent protein (GFP)–RGA fusion protein from root cell nuclei via a constitutive triple response 1 (CTR1)-dependent signalling pathway (Achard *et al.*, 2003). Furthermore, ethylene was shown to control the maintenance and exaggeration of the apical hook by modifying DELLA degradation (Achard *et al.*, 2003; Vriezen *et al.*, 2004). More recently, it was demonstrated that active ethylene signalling results in decreased GA content, thus stabilizing DELLA proteins (Achard *et al.*, 2007). Hence, ethylene appears to affect DELLA stability primarily via changes in GA concentrations.

In order to reveal how the modulation of ethylene and GA pathways affects global plant growth, the effects of simultaneous alterations in these pathways were assessed at the whole-plant level. In this work, we present the characterization of the gibberellin-insensitive (*gai*), ethylene-overproducing 2-1 (*eto2-1*) double mutant, which is negatively affected in GA signalling and positively affected in ethylene biosynthesis. These two effects (reduced GA signalling and enhanced ethylene accumulation) both limit cell expansion. The (semidominant) gain-of-function mutant *gai* encodes a protein lacking a segment of 17 amino acids from close to the N-terminus, resulting in a reduced response to GAs which cannot be rescued by application of the hormone, as well as an elevated endogenous GA concentrations. The latter arises from loss of feedback regulation, inducing transcription of GA-biosynthesis genes (GA 20-oxidase and GA 3β-hydrolase) (Talon *et al.*, 1990; Cowling *et al.*, 1998). The ethylene-overproducing *eto2-1* mutant has a single base pair insertion, disrupting the C-terminal 12 amino acids of 1-aminocyclopropane-1-carboxylic acid (ACC) synthase 5 (*ACS5*), one of the nine *ACS* genes in Arabidopsis (Vogel *et al.*, 1998; Chae & Kieber, 2005). The C-terminal region is necessary for proteolytic targeting of ACS5 in wild type; hence, the truncated form of ACS5 in *eto2-1* is more stable. Although dark-grown seedlings produced approximately 20 times more ethylene than the wild type, adult tissues from *eto2-1* mutants and light-grown *eto2-1* seedlings had a concentration of ethylene that was only slightly higher than that of wild-type tissues (Vogel *et al.*, 1998). Therefore, both the developmental stage and the presence of light appear to affect ACS5 activity.

In order to determine the combined effects of the *gai* and *eto2-1* mutations, the growth and development of the double mutant were compared with those of the single-mutant parents and the wild type throughout the entire life-cycle, from hypocotyl growth until flowering. Root and shoot growth were assessed by *in vivo* imaging, revealing an enhanced shoot:root ratio in the double mutant. Growth inhibition seems to be synergistic in the double mutant, as does floral induction. In addition, ethylene and GA concentrations were measured in all genotypes. Our results indicate that altered GA sensitivity in the *gai eto2-1* double mutant, which has an elevated GA content as a consequence, may cause the observed growth alterations through changes in ethylene responsiveness.

Materials and Methods

Plant material and growth conditions

Wild-type Columbia (Col-0) *Arabidopsis thaliana* (L.) Heynh. was obtained from the Nottingham Arabidopsis Stock Centre. The Arabidopsis mutants *eto2-1* and *gai1* were obtained from the Arabidopsis Biological Resource Centre at Ohio State University. Because *eto2-1* is in the Columbia and *gai1* in the Landsberg *erecta* (Ler) background, *gai1* was crossed four times with Col-0 to obtain a *gai* mutant theoretically containing > 93% Columbia genotype. This *gai* mutant was used in all experiments and subsequent crosses.

Except for the hypocotyl measurements and the flowering time experiment, all plants were grown on Murashige and Skoog (MS)/2 medium +1% sucrose. Seeds were imbibed at 4°C for 2 d. Plantlets were grown in continuous light at 21°C, and at a photosynthetic photon flux density of 75 μmol m^{-2} s^{-1}. For hypocotyl measurements, seedlings were grown on low nutrient medium (LNM; Smalle *et al.*, 1997) at 22°C in 16 h light : 8 h dark, and with a photosynthetic photon flux density of 54 μmol m^{-2} s^{-1}. ACC, aminoethoxyvinylglycine (AVG) and GA_3 were purchased from Sigma (St Louis, MO, USA). AVG at a concentration of 1 μM (dissolved in water) and a variable concentration of ACC or GA_3 (dissolved in ethanol) were added to the medium. Seeds were imbibed at 4°C for 2 d. Dark-grown seeds were grown at 22°C, after 2 h of exposure to white fluorescent light (130 μmol m^{-2} s^{-1}) to stimulate germination.

For the flowering time experiment, seeds were sown directly on Jiffy's (Jiffy, Drøbak, Norway) and watered with 50 ml/100 l Wuxal super 8-8-6 (OptimAgro, Diegem, Belgium)

nutrients. Plants were grown on soil at 22°C in 16 h light : 8 h dark, at a photosynthetic photon flux density of 54 μmol m^{-2} s^{-1}. Ethylene treatments were essentially as described previously (Achard *et al.*, 2006; treatments with 1 ppm ethylene (Air Liquide, Liège, Belgium)).

The same conditions were used to grow plants for GA measurements with a photosynthetic photon flux density of 130 μmol m^{-2} s^{-1}.

Construction of the *gai eto2-1* double mutant

gai (Col-0 background) was crossed with *eto2-1*. Dark-green plants with a triple response in the absence of ethylene were selected from the F2. Double-homozygous individuals were identified from this population by analysing the F3. Homozygosity for *gai* was confirmed by PCR amplification of a DNA fragment using the oligonucleotides gaifw1: 5′-ATGAAGAAGACGACGGTAATGG-3′ and gairev1: 5′-TAGCGAACTGATTGAGAATCGC-3′ in a PCR reaction consisting of 30 cycles of 30 s at each of 95, 50 and 72°C. DNA from homozygous *gai* plants led to the production of a 239-bp fragment, whereas DNA from plants heterozygous for *gai* yielded two fragments, one of 290 bp and one of 239 bp. *eto2-1* homozygosity was checked by a DNA restriction digestion: as only mutated plants contain an *Ava*I or *Sma*I site in *AtACS5*, PCR was performed, using the oligonucleotides ACS5-1: 5′-GAAGCAGAGCTTGACCTCTGG-3′ and ACS5-2: 5′-GTTCGTCGTCTCAAACTTAGGG-3′ and the fragments obtained were digested using *Ava*I. Wild-type plants contained one fragment of 327 bp, homozygous *eto2-1* plants showed two bands, one at 255 bp and one at 72 bp, and heterozygous plants yielded all three fragments. As a final control, sequences of double-homozygous plants were checked.

Root growth measurements

An initial root growth experiment was performed on plants grown on vertical plates, and root length was scored every 24 h. Hypocotyl and root lengths were measured as described by Smalle *et al.* (1997), using a Stemi SV 11 microscope (Zeiss, Cologne, Germany). Plants were photographed and hypocotyls were measured using ImageJ (http://rsb.info.nih.gov/ij/). At 8 and 15 d after germination, primary lateral roots were counted.

Kinematic analyses were performed 8 or 15 d after germination of vertically placed seedlings. For this purpose, a series of overlapping time-lapse images were obtained that covered the entire growth zone using a ×5 lens on a vertically oriented microscope (Axiolab; Zeiss) with a charge-coupled device camera connected to a PC fitted with a Scion LC3 framegrabber board and ScionImage software (Scion, Frederick, MD, USA). For each treatment, at least three replicate roots were imaged nine times at 10-s intervals. The image stacks obtained were used for calculation of velocity and strain rate profiles using RootflowRT software (van der Weele *et al.*, 2003).

Shoot growth measurements

For the analysis of shoot growth, plants were grown on horizontal plates for 15 d. A chlorophyll fluorescence imaging system was used to measure leaf expansion. The system consists of a miniature black and white CCD camera with < 0.1 Lux sensitivity, fitted with a cut-off high-pass surrounded by a ring of six small halogen lamps, shielded by a blue cut-off low-pass filter (Scott BG-39; Scott, Lancashire, UK) to provide excitation light below 650 nm (Chaerle *et al.*, 2004). Arabidopsis plants were illuminated with 250 μmol m^{-2} s^{-1} blue light for 1 s; subsequently the chlorophyll fluorescence image was captured. At the start of the experiment, the robotized measuring system, which carries out the chlorophyll fluorescence imaging, was programmed to obtain images of all seedlings. Subsequently, images were captured automatically at intervals of 6 h. The ImageJ area calculator plug-in was used to quantify leaf area, using the same threshold for all images.

Shoot:root ratios

Plants were grown on horizontal plates. After 8, 10, 12 or 15 d, shoots and roots were separated and pools of at least 10 plants were blotted between tissue paper, dried under pressure for 4 d at room temperature and weighed (Narang *et al.*, 2000)

Ethylene emanation

For ethylene measurements, a minimum of 20 seeds were sterilized and sown in 10-ml glass vials (Chrompack, Middleburg, the Netherlands), containing 5 ml of MS/2 medium, and sealed with white gas-porous tape (Urgopore, Chenoves, France). Plants were grown in continuous light conditions as described in the section 'Plant material and growth conditions' above. After 8 and 15 d, respectively, the vials were capped with a gas-tight seal. After 75 min of accumulation, the ethylene emanation was measured. Ethylene analysis was carried out on an ETD-300 laser-based photo-acoustic ethylene detector equipped with a valve control box (Sensor Sense, Nijmegen, the Netherlands). Data acquisition was performed with OriginPro 7.5 software (OriginLab Corporation, Northhampton, NH, USA). Three independent series of experiments were carried out with at least three measurements each.

GA content

Samples corresponding to approx. 0.2 g fresh weight were first homogenized in liquid nitrogen with a mortar and pestle, and thereafter extracted in 3 ml of 80% methanol with 0.02% diethyl dithiocarbamate as antioxidant with vigorous shaking for 2 h at 4°C. Deuterated GAs ([17,17-$^2H_2$]GA) were added as internal standards (provided by Professor L. Mander, Australian National University Canberra, Australia) before extraction. The mixture was centrifuged at 700 ***g*** for 10 min at

4°C. The supernatant was transferred into Kimble tubes and dried under reduced pressure. The pellet was redissolved in 50 µl of methanol. Hexane (300 µl) was added and the mixture was applied to a Silica (1 g) Isolute cartridge (Sorbent AB, V. Frölunda, Sweden) previously conditioned with hexane and balanced with hexane/ethyl acetate (80 : 20). The column was washed with hexane/ethyl acetate (80 : 20) and GAs were eluted with methanol containing 1% acetic acid. The methanol eluate was dried and, after methylation with ethereal diazomethane, the samples were subjected to reverse-phase high-performance liquid chromatography (HPLC).

The HPLC system consisted of a Waters model 600 pump (Waters Associates, Milford, MA, USA) connected via a Waters 717 autosampler to a 4-µm Symmetri C_{18} column (150 mm × 3.9 mm i.d.; Waters Associates). The mobile phase was a 20-min linear gradient of 30–100% methanol in 1% aqueous acetic acid at a flow rate of 1 ml min^{-1}. Five fraction corresponding to the GAs of interest were dried, and after evaporation trimethylsilylated in 20 µl of dry pyridine:BSTFA: trimethylchlorosilane (50 : 50 : 1, volume/volume (v/v)) at 70°C for 30 min. The derivatization mixture was then reduced to dryness and dissolved in 15 µl of heptane. Samples were injected in the splitless mode into an HP 5890 gas chromatograph (Hewlett Packard, Palo Alto, CA, USA) fitted with a fused silica glass capillary column (30 m long, 0.25 mm i.d.) with a chemically bonded 0.25-µm DB-5MS stationary phase (J & W Scientific, Folsom, CA, USA). The injector temperature was 270°C. The column temperature program varied depending on which GA was being analysed. The column effluent was introduced into the ion source of a JMS-SX/SX102A mass spectrometer (JEOL, Tokyo, Japan). The interface temperature was 270°C and the ion source temperature 250°C. The acceleration voltage was 10 kV, and ions were generated with 70 eV at an emission current of 500 µA. For quantification, samples were analysed in selected reaction monitoring mode (SRM) (Moritz & Olsen, 1995). All data were processed using a JEOL MS-MP7010 data system.

Real-time quantitative PCR (qPCR)

Total RNA was isolated using an RNeasy Plant Mini Kit (Qiagen, Venlo, the Netherlands). Total RNA (3 µg) was treated with DNaseI (Turbo DNA-free kit; Ambion, Austin, TX, USA) and 0.5 µg was used as a template to synthesize cDNA using the SuperScript III Platinum Two-Step qRT-PCR Kit with SYBR Green (Invitrogen, Paisley, UK). Gene-specific primers were designed using Primer Express version 2.0 (Applied Biosystems, Foster City, CA, USA) or GENOPLANTE SPADS software (http://urgi.infobiogen.fr/tools/spads/) and are listed in Supplementary Material Table S1. PCR reactions were performed on an ABI 7500 Real Time PCR System (Applied Biosystems) using Platinum SYBR Green qPCR SuperMix-UDG reagents (Invitrogen), according to the manufacturer's specification, with the cDNA equivalent of 10 ng of RNA in a 25-µl reaction volume. Reactions were performed in triplicate and the absence of genomic DNA and primer dimers was confirmed by analysis of reverse-transcriptase (RT)-minus and water control samples and by examination of dissociation curves. Analysis of the amplification curves with LINREG software (Ramakers *et al.*, 2003) showed that the efficiency of each PCR primer pair was above 0.95. Data were normalized using ubiquitin conjugating enzyme (UBC) transcripts as the reference; there was no sign of regulation of UBC in any of the mutants. Relative quantities were calculated with QBASE version 1.3.4 software (http://medgen.ugent.be/qbase/), taking the estimated efficiency of each primer pair into consideration.

Results

gai and *eto2-1* mutations affect root growth rates

Roots of *gai*, *eto2-1* and *gai eto2-1* mutants, grown on vertical plates for 17 d, grew more slowly than wild-type roots, indicating that root growth is influenced by the mutations in both the ethylene and the GA pathways (Fig. 1a). Although the velocity of growth was greatest for wild type, the growth patterns of Col-0, *gai* and *eto2-1* were comparable, showing acceleration in growth rate until 8 d after germination (DAG), after which a plateau was reached (no significant differences between two consecutive measurements were noted in any of these genotypes from day 8 onwards; Student's *t*-test: $P > 0.01$). In contrast, roots of *gai eto2-1* showed the same acceleration in growth in young seedlings, but after reaching maximum growth at 8 DAG, their growth rate dropped drastically (Fig. 1a). Moreover, as the growth rate at 15 DAG was reduced to 93% of the wild-type rate for *gai*, and to 64% for *eto2-1* and 30% for the double mutant, this suggests that the *gai* and *eto2-1* mutations have a synergistic effect on root growth at this stage of development.

To examine the observed differences in growth rate at the cellular level, a kinematic analysis at different stages of plant development was performed. As 8 DAG seems to be crucial in the development of *gai eto2-1*, this stage was analysed in more detail, as was growth at 15 DAG, when most lines are growing at relatively constant rates. Both velocity and relative (strain) rates of cell expansion along the elongation zone were calculated using ROOTFLOWRT software (van der Weele *et al.*, 2003). The velocity profile typically follows an S-shape curve, with slow rates at the tip, followed by a region of rapid increase, and finally a constant rate in the remaining, mature part of the root. This constant rate equals the growth rate of the root. The derivative of this curve reveals local rates of cell expansion (Fig. 1b).

Results shown in Fig. 1(a) indicate that, at 8 DAG, roots of Col-0 had the highest growth rate, followed by roots of *gai* and *gai eto2-1*, which showed no significant differences (Student's *t*-test: $P = 0.2346$), while *eto2-1* was growing most slowly. These results are confirmed by the kinematic data

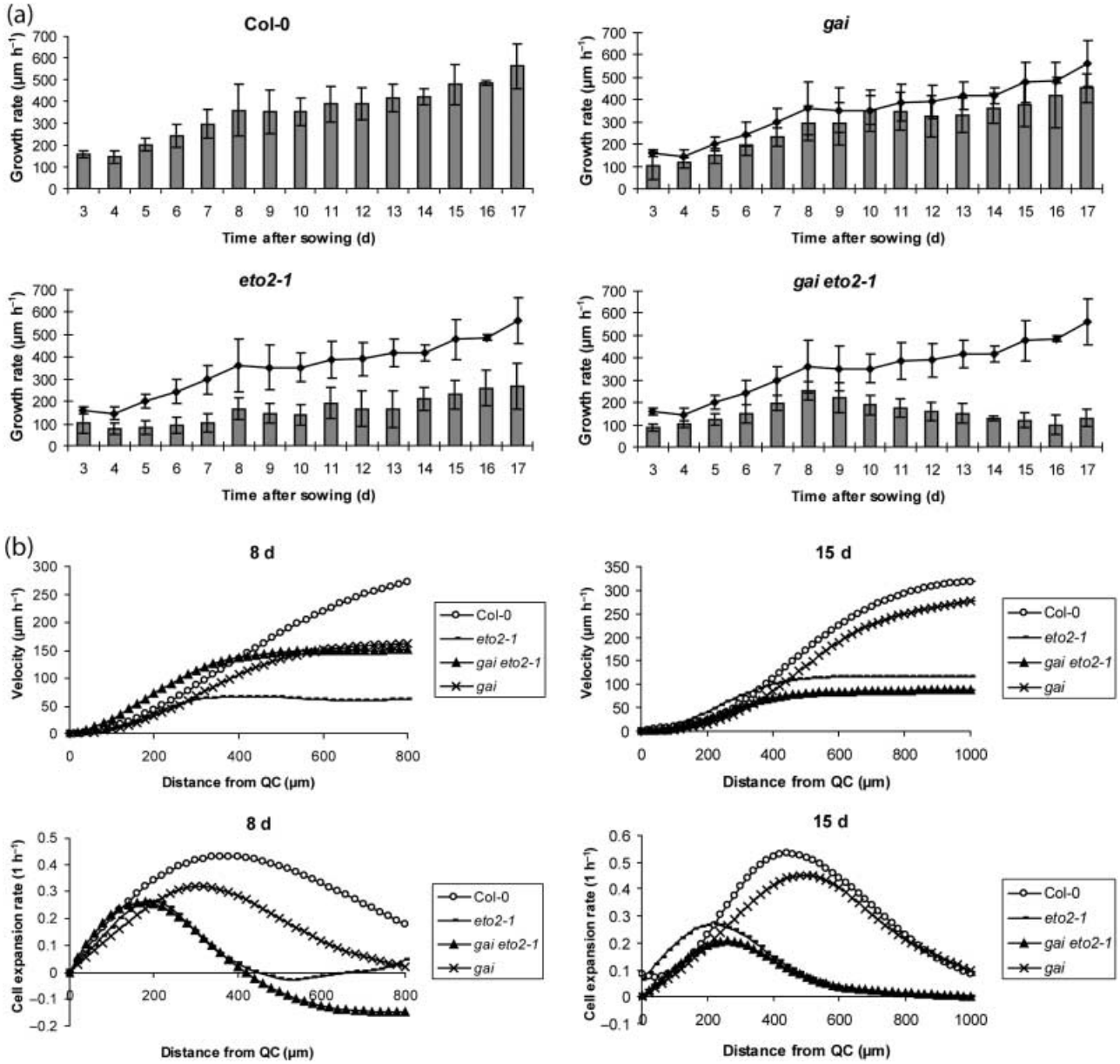

Fig. 1 Kinematic analysis of root growth of Columbia (Col-0), and gibberellin-insensitive (*gai*), ethylene-overproducing 2-1 (*eto2-1*) and *gai eto2-1* mutants. Arabidopsis seedlings were grown on vertical plates in continuous light. (a) Root length was measured every 24 h. Graphs show additional growth in 24 h until 17 d after germination (DAG). Line graphs superimposed on the bar graphs of mutants represent the Col-0 root growth; error bars represent ± SD. (b) Profiles of velocity and relative rates of cell expansion of 8- and 15-d-old seedlings, measured from the quiescent centre (QC). Graphs represent averages of at least five plants.

obtained in the RootflowRT analysis (Fig. 1b). At 15 DAG, the growth of *gai* increased to the wild-type level, while the growth rate of *gai eto2-1* decreased to a level below that of *eto2-1*, as observed in Fig. 1(a,b). Typically, the length of the growth zone of *in vitro* grown roots increases over time (Beemster & Baskin, 1998). Consistent with this, as the maximum in cell expansion rate was shifted, the growth zone was increased between 8 and 15 DAG for *gai* and Col-0. The enlargement of the elongation zones of *gai eto2-1* and *eto2-1* was minimal, which is in agreement with the total root length and growth rate results.

Differences in root growth rates are attributable to cell elongation, not cell division

For a more detailed view of root development, roots of all mutants were studied in their totality as well as at the cellular level at the stages already mentioned (8 and 15 DAG).

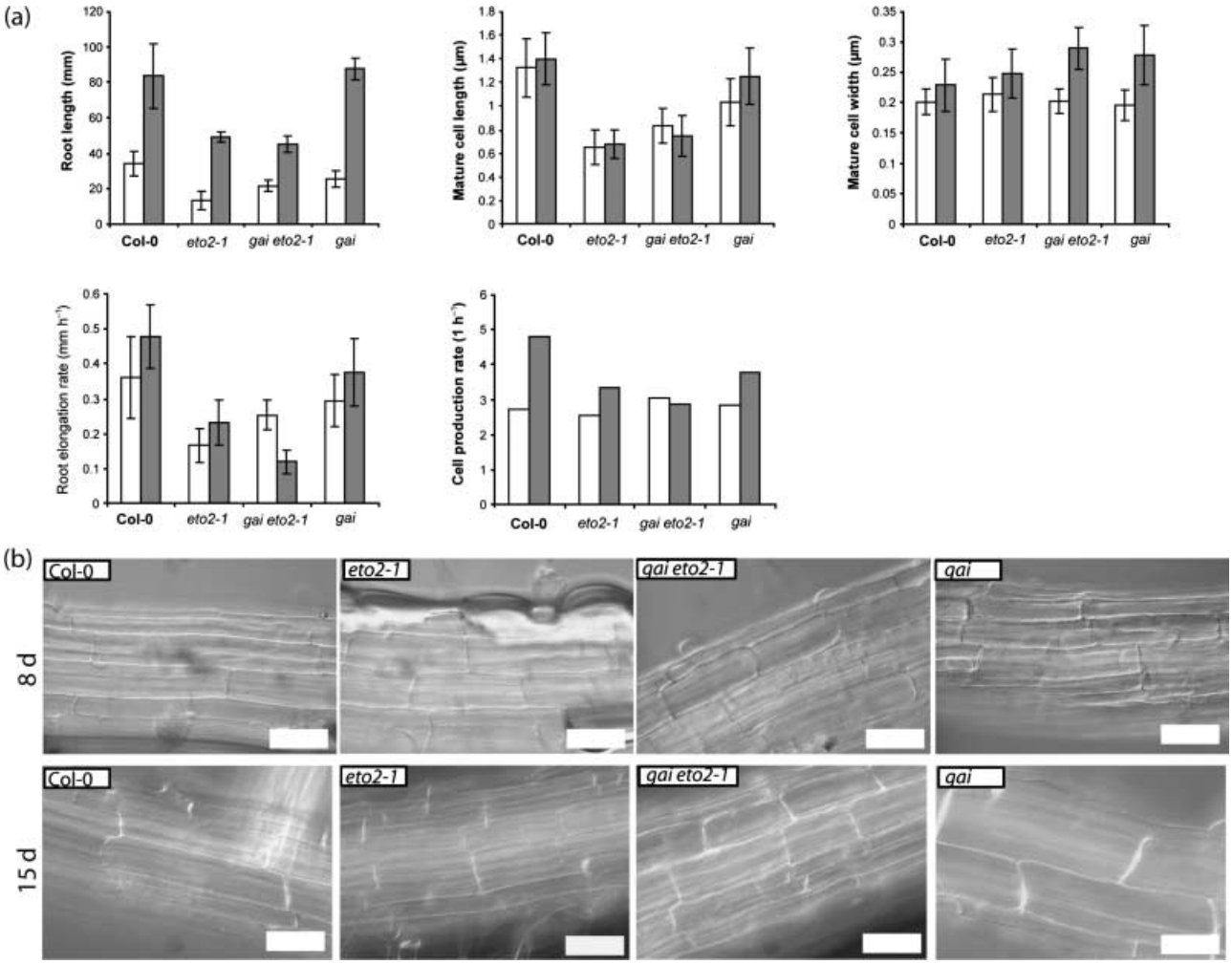

Fig. 2 (a) Biometric analysis of roots of 8-d-old (open bars) and 15-d-old (closed bars) Arabidopsis Columbia (Col-0), gibberellin-insensitive (*gai*), ethylene-overproducing 2-1 (*eto2-1*) and *gai eto2-1* seedlings grown in continuous light. Top left panel, total root length; top middle panel, cell length; top right panel, cell width. Bottom left panel, root elongation rate; bottom right panel, cell production rate. In all graphs, error bars represent ± SD. (b) Microscope images of mature cells of 8-d-old (upper row) and 15-d-old (lower row) seedlings. Bars, 40 μm. Pictures were taken of epidermal cells just above the root-hair elongation zone.

Measurements of the root lengths showed that the roots of *gai eto2-1* were initially intermediate between the roots of the two single mutants but had the same length as *eto2-1* roots at 15 DAG (Fig. 2a). Because of the faster growth of *eto2-1* at this stage (Fig. 1a,b), the *gai eto2-1* root became clearly the smallest after 17 d (data not shown).

To assess the effects of the mutations on growth of individual cells, mature cell lengths were measured at 8 and 15 DAG (Fig. 2a). These data showed the exact same patterns as data for the total root length and growth rates of the same plants. Measurements of the root cell width did not show this pattern, suggesting that the difference in total root length is mainly attributable to a change in longitudinal cell expansion. As root elongation is proportionate to the mature cell length and to the cell production rate, the latter could be calculated. These results indicate that, at 8 DAG, the differences in cell production rate were rather small among all phenotypes. At 15 DAG, the cell production rate of Col-0 and *eto2-1* accelerated, while that of *gai* was still comparable with that at 8 DAG. The cell production rate of *gai eto2-1* dropped after 15 DAG (Fig. 2a). These data show that the reduced root length of *gai eto2-1* is caused by a combination of inhibition of cell elongation and cell production.

Effects on lateral root formation

It is possible that the enhanced root phenotype noted in *gai eto2-1* is a result of a loss of primary-root dominance, thereby enhancing lateral root development. To determine whether lateral root formation was changed in the double mutant, the number of lateral roots was examined at 8 and 15 DAG (Fig. 3).

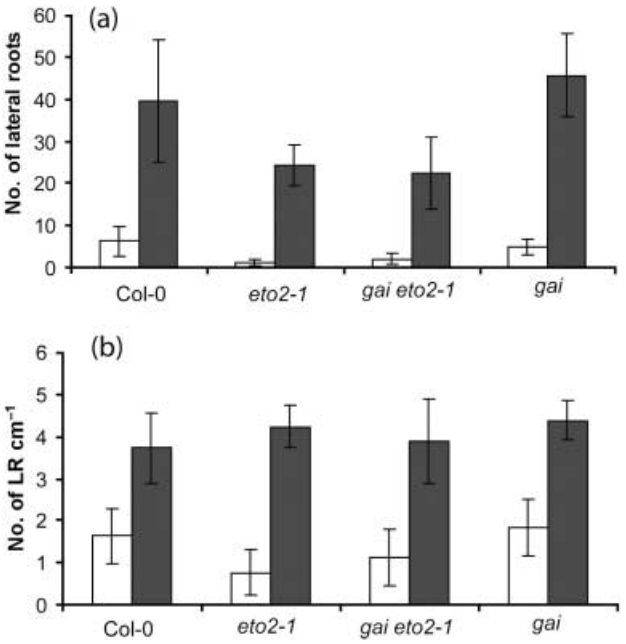

Fig. 3 Analysis of lateral roots of 8-d-old (open bars) and 15-d-old (closed bars) Arabidopsis Columbia (Col-0), gibberellin-insensitive (*gai*), ethylene-overproducing 2-1 (*eto2-1*) and *gai eto2-1* seedlings grown in continuous light. (a) Number of lateral roots (primary branching). (b) Relative number of lateral roots, expressed as number of lateral roots (LR) per cm of primary root. Error bars, ± SD.

In terms of absolute number of lateral roots, there were not many differences between the plants at 8 DAG as compared with 15 DAG. At 8 DAG, the number of lateral roots was smallest for *eto2-1*, followed by the double mutant, *gai* and Col-0, respectively. At 15 DAG this order was maintained, but the differences between *eto2-1* and *gai eto2-1* and between Col-0 and *gai* were no longer significant (Student's *t*-test, $P > 0.01$) (Fig. 3a).

When the number of lateral roots was expressed on a per cm basis to take into account differences in primary root length, a comparable result as for the absolute number of lateral roots was observed at 8 DAG. At 15 DAG, however, the number of lateral roots per cm was comparable for all mutants (Fig. 3b). As *eto2-1* and *gai eto2-1* have smaller roots than wild type and *gai*, these results indicate that the *eto2-1* background causes a greater production of lateral roots between 8 and 15 DAG. As comparable lateral root formation was seen in *gai eto2-1* and *eto2-1*, this phenotype could not be responsible for the relative reduction in growth rate of the roots in the double mutant. In addition, measurement of lateral root length showed that *gai eto2-1* did not have longer lateral roots as compared with the single mutants or the wild type (data not shown).

Both *eto2-1* and *gai* are affected in shoot growth

Another possible explanation for the reduced root growth rate noted in the double mutant could be that, at a certain stage, the plant allocated more energy towards shoot development, thereby neglecting root growth. To determine whether shoot growth is also altered in the double mutant, shoots of plants grown on horizontal plates in continuous light were imaged every 24 h until 15 DAG (Fig. 4). Based on these top-view pictures, shoot enlargement was calculated on a daily basis. Although the growth rate was highest in Col-0, shoots of wild type and both single mutants developed in a similar manner: the increment in shoot growth increased every day, with a large enhancement at around day 12. By contrast, shoot enlargement of *gai eto2-1* reached a maximum at 10 DAG and remained stable until 12 DAG, after which it dropped severely (Fig. 4a). As for total root length (Fig. 2), the surface area of *gai eto2-1* shoots at 15 DAG was smaller (19% of the wild-type value) than that of both single mutants (*eto2-1* being larger than *gai*; respectively, 45 and 39% of the wild-type value), while Col-0 developed the largest shoots (Fig. 4b,c). These data indicate that the *gai* and *eto2-1* mutations also have a synergistic effect on shoot growth.

To further assess the relationship between root and shoot growth, the dry weights of shoots and roots were compared at some critical time-points (8, 10, 12 and 15 DAG). Figure 5 shows that the shoot:root ratio of Col-0 and *gai* did not vary much during the time-course. By contrast, the shoot:root ratio for both *eto2-1* and *gai eto2-1* was increased at 15 DAG. However, the shoot:root ratio of *eto2-1* remained stable until day 12 and increased only at day 15. For *gai eto2-1*, the shoot:root ratio started to increase at 9 DAG, reaching a maximum after 10 d and remaining at the same value thereafter (Fig. 5). In conclusion, these results indicate a redirection of the energy of the plant to shoot growth in *gai eto2-1*, which causes suppression of root development.

Floral transition is significantly delayed in *gai eto2-1*

To assess whether the observed alteration in shoot growth has an influence on floral behaviour, flowering time in long day (LD) conditions was recorded as days to flowering and as number of leaves in the vegetative rosette to bolting, both in an ethylene-free and in an ethylene-enriched environment (Fig. 6a). Ethylene has been shown previously to delay flowering of wild-type plants (Achard *et al.*, 2006). All mutants were significantly delayed as compared with wild type when grown without ethylene (3, 19 and 17 d for *eto2-1*, *gai eto2-1* and *gai*, respectively, corresponding to 5, 20 and 15 leaves more than the wild type upon bolting). As for the wild type, ethylene caused a further delay in floral induction (11, 23 and 14 d, corresponding to 10, 22 and 14 leaves for *eto2-1*, *gai eto2-1* and *gai* as compared with the respective untreated controls). However, when the relative increase in bolting time was considered (Fig. 6b), the delay was most severe in the wild type. Surprisingly, the relative increase was larger in *gai eto2-1* than in either of the single mutants, when expressed both as days to flowering and as number of leaves at bolting,

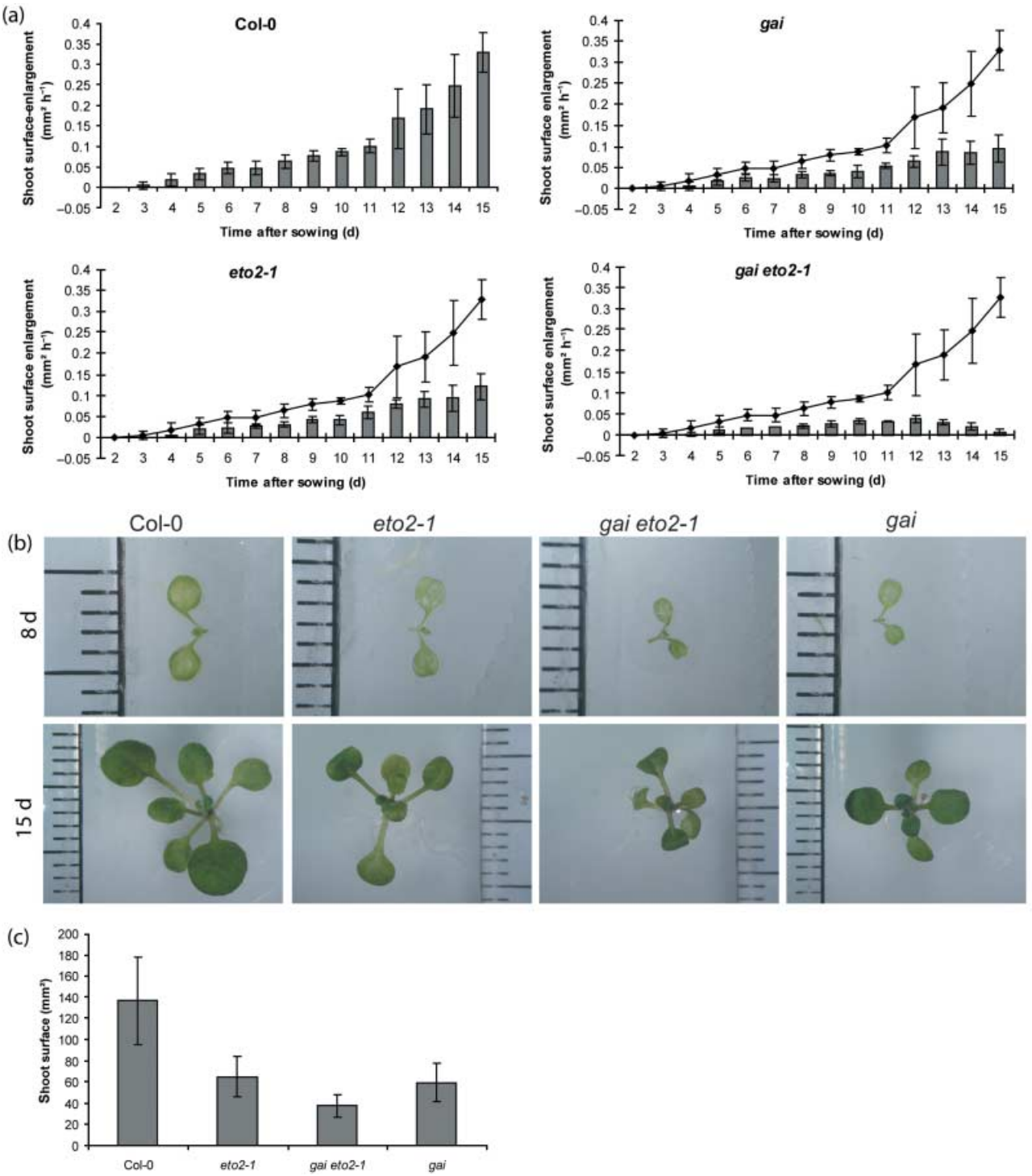

Fig. 4 Kinematic analysis of shoot growth. Columbia (Col-0), gibberellin-insensitive (*gai*), ethylene-overproducing 2-1 (*eto2-1*) and *gai eto2-1* seedlings were grown in continuous light for 15 d, and measurements of shoot surfaces were made every 24 h. (a) Bar graphs of shoot surface enlargement as a function of time ($mm^2\ h^{-1}$). Line graphs superimposed on the bar graphs of mutants represent the Col-0 shoot growth; error bars represent ± SD. (b) Images of shoots of representative 8- and 15-d-old light-grown plants. (c) Total shoot surface of 15-d-old plants. Error bars, ± SD.

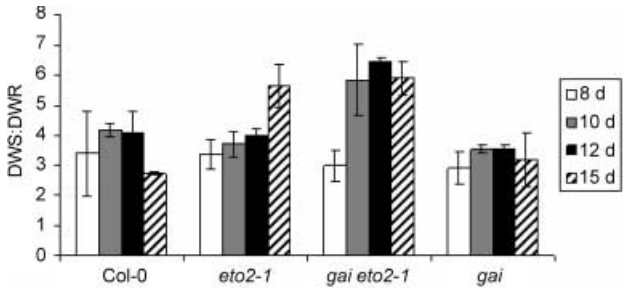

Fig. 5 Shoot–root relations in Columbia (Col-0), gibberellin-insensitive (*gai*), ethylene-overproducing 2-1 (*eto2-1*) and *gai eto2-1*. Arabidopsis seedlings were grown in continuous light. The dry weights of roots (DWR) and shoots (DWS) were measured at different stages (8, 10, 12 and 15 d). Graphs show shoot:root ratios (DWS:DWR).

indicating that; although the *gai* mutation is the major contributor to the late-flowering phenotype, the observed effect on floral delay upon ethylene treatment is caused by a combination of the two mutations. In addition, when ethylene emanation of bolting plants was measured (Supplementary Material Fig. S1), a significantly higher production was noted in *gai eto2-1* as compared with that in the *gai* mutant.

The total length of the inflorescence was measured in adult plants (55 DAG) (Supplementary Material Fig. S2). The results show that the total length of *gai eto2-1* was significantly lower than that of the single mutants (Student's *t*-test, $P < 0.01$). Thus, an additive effect in inflorescence length was seen in the *gai eto2-1* mutant compared with both single mutants.

The enhanced ethylene production of *eto2-1* is suppressed in the gibberellin-insensitive background of the double mutant

As ethylene is known to reduce cell expansion (Kieber *et al.*, 1993; Rodrigues-Pousada *et al.*, 1993) and to confirm the effect of *eto2-1* on ethylene production, we measured ethylene emanation from single and double mutants (Fig. 7). Despite an earlier report that light-grown *eto2-1* produces ethylene at concentrations no more than 30% above those of the wild type (Vogel *et al.*, 1998), we reproducibly found a 4-fold higher ethylene emanation in the *eto2-1* mutant as compared with Col-0. In contrast, no differences were found in ethylene emanation between the wild type and the *gai* mutant. Remarkably, the enhanced ethylene production caused by the *eto2-1* mutation was not seen in the *gai eto2-1* double mutant.

Enhanced responsiveness towards ethylene may explain the *gai eto2-1* phenotype in the light

As the synergistic growth inhibition phenotype of *gai eto2-1* roots could not be explained by an enhancement of ethylene production, ethylene responsiveness was assessed in a hypocotyl elongation assay in light- and dark-grown seedlings. Application of ethylene or its precursor ACC causes hypocotyl elongation in the light and inhibition of hypocotyl growth in the dark (Smalle *et al.*, 1997). To exclude the influence of endogenous synthesis of ethylene, an ethylene-biosynthesis inhibitor, aminoethoxyvinylglycine (AVG), was added to the medium, together with an increasing concentration of ACC, and plants were grown for 8 d in long-day conditions (16 h light/8 h dark) (Fig. 8). The dose–response curve shows that the *gai eto2-1* double mutant had an enhanced ethylene response, indicated by longer hypocotyls at low concentrations of ACC (0.1–0.5 μM), when compared with the wild-type and both single mutants. This tendency of enhanced responsiveness at low ACC concentrations (up to 0.1 μM) was also found when silver thiosulphate was used to block ethylene action (data not shown). In darkness, however, no difference in responsiveness was observed (data not shown).

GA production is enhanced in young seedlings of the double mutant

In addition to the ethylene-production measurements, the GA content of seedlings (13 DAG) was analysed (Fig. 9). These results indicated that the active form GA_4 and its biosynthetic precursor GA_{24} (non-13-OH pathway) accumulated to higher concentrations in the double mutant compared with the other genotypes. The content of GA_9, the direct precursor of GA_4, and GA_{34}, an inactive GA_4 metabolite, were as high in the double mutant as in *gai*, but both were higher than in the wild type and in *eto2-1* (Fig. 9). None of the GA species derived from GA_{53} (the 13-OH pathway) showed a clear difference among the wild type and the single and double mutants, except for the inactive GA_8, which was higher in *gai* and the double mutant.

In rosette-stage plants (the eight-leaf stage), the same patterns were seen as in seedlings, except that the GA_{24} content of *gai eto2-1* was not as high as the content measured in seedlings (Supplementary Material Fig. S3).

Enhanced GA production is partially confirmed by expression patterns of GA-biosynthesis genes

In addition to analysis of GA content, expression patterns of well-described GA-biosynthesis genes were analysed in plants of the same age, 13 DAG (Fig. 10). For *ent*-copalyl diphosphate synthase (CPS), which catalyses the first step of GA biosynthesis (Sun *et al.*, 1992), expression was highest in *gai*. Transcript levels of gibberellin-20-oxidases (*GA20ox*) were much increased in both *gai* and *gai eto2-1*. Apart from *GA20ox1*, expression of these genes was lower in *eto2-1* than in wild type. For *GA3ox1*, expression in the ethylene-overproducing mutant was slightly higher than in the wild type; however, both products accumulated to levels far below those found in *gai* and in the double mutant. The two *GA2ox* genes analysed showed a similar pattern, with the highest expression in Col-0 and no significant differences among all mutants (Fig. 10).

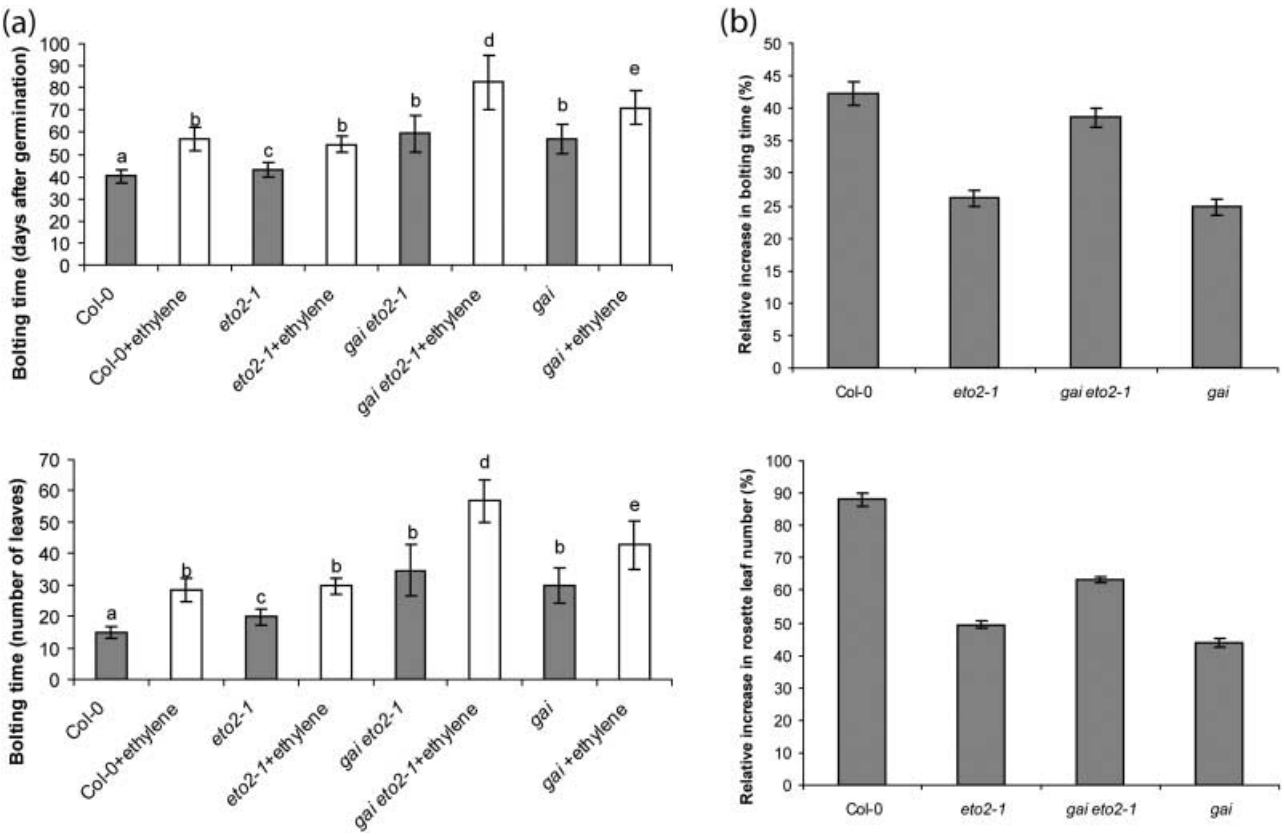

Fig. 6 Comparison of flowering of Arabidopsis Columbia (Col-0), and gibberellin-insensitive (*gai*), ethylene-overproducing 2-1 (*eto2-1*) and *gai eto2-1* mutants. (a) Bolting time parameters of wild type and mutants (*gai*, *eto2-1* and *gai eto2-1*) grown in the absence (closed bars) or presence (open bars) of ethylene. Flowering time was expressed temporally (days) or as the number of vegetative leaves produced before flowering. Letters above bars indicate significant differences between treatments (Student's *t*-test: $P < 0.05$): bars with the same letter represent data with no significant difference. (b) Mean relative increase in bolting time and number of rosette leaves upon ethylene treatment, expressed as a percentage of the untreated control. Error bars, ± SD.

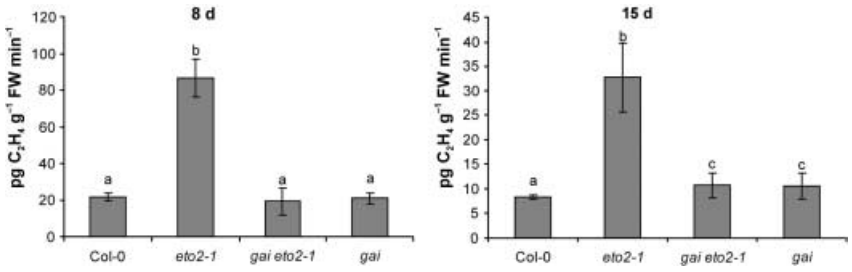

Fig. 7 Ethylene emanation (pg C_2H_4 g^{-1} FW min^{-1}) from 8- and 15-d-old Arabidopsis Columbia (Col-0), gibberellin-insensitive (*gai*), ethylene-overproducing 2-1 (*eto2-1*) and *gai eto2-1* seedlings. Plants were grown in 10-ml cuvettes in continuous light. Error bars represent ± SD. Different letters represent significantly different values (Student's *t*-test: $P < 0.001$): the same letters represent data with no significant difference.

GA responsiveness is comparable between *gai eto2-1* and *eto2-1*

We further analysed differences in GA responsiveness among the different genotypes. To that end, the hypocotyl elongation of light-grown seedlings in response to GA was measured. Plants were grown for 8 d in long-day conditions (16 h light : 8 h dark) in a medium supplemented with various concentrations of GA_3 (Fig. 11). The results show that the double mutant significantly responded to GA treatment, in contrast to *gai*, which was insensitive to applied GA.

Discussion

The phenotypic plasticity of a plant is achieved by integration of environmental and internal signals, collectively orchestrating output at the transcriptome and proteome level, resulting in an optimal growth response (Vandenbussche & Van Der Straeten, 2004). Several of these responses involve crosstalk between the ethylene and GA signalling pathways. The most conspicuous example of such an interaction is the extension growth of deepwater rice (*Oryza sativa*) upon submergence (Kende *et al.*, 1998; Vriezen *et al.*, 2003). In addition to

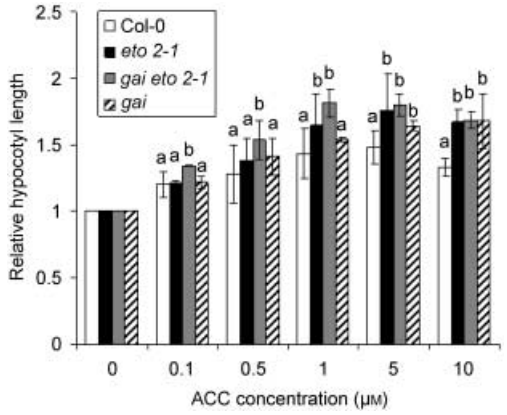

Fig. 8 1-aminocyclopropane-1-carboxylic acid (ACC) dose–response curve for hypocotyl length of 8-d-old light-grown Arabidopsis seedlings. Wild-type and mutant seedlings (gibberellin-insensitive (*gai*), ethylene-overproducing 2-1 (*eto2-1*) and *gai eto2-1*) were grown in long-day conditions (16 h light : 8 h dark) on low-nutrient medium supplemented with 1 μM aminoethoxyvinylglycine (AVG) and an increasing concentration of ACC. Graphs represent relative hypocotyl length; error bars represent ± SD. Letters above bars indicate a significant difference within concentrations (Student's *t*-test: $P < 0.05$): the same letters represent data with no significant difference within the treatment.

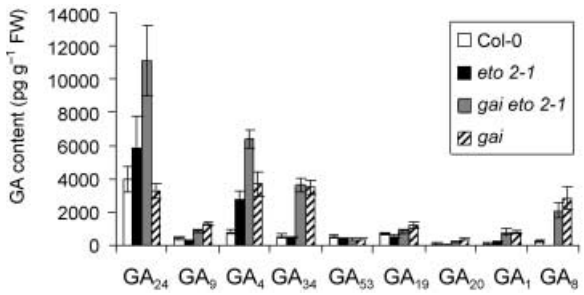

Fig. 9 Gibberellin (GA) content in young Arabidopsis seedlings of Columbia (Col-0), gibberellin-insensitive (*gai*), ethylene-overproducing 2-1 (*eto2-1*) and *gai eto2-1*. Plants were grown under long-day conditions until 13 d after germination. Error bars, ± SD.

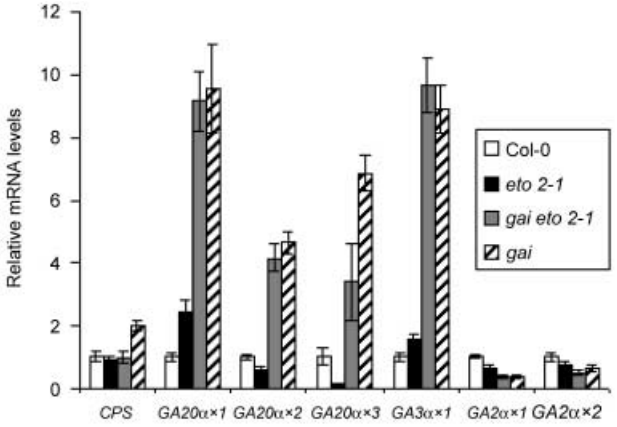

Fig. 10 Expression of gibberellin (GA)-biosynthesis genes in Arabidopsis Columbia (Col-0), gibberellin-insensitive (*gai*), ethylene-overproducing 2-1 (*eto2-1*) and *gai eto2-1* seedlings determined using quantitative PCR. Plants were grown under long-day conditions until 13 d after germination. Error bars, ± SD. *CPS*, *ent*-copalyl diphosphate synthase; *ox*, oxidase.

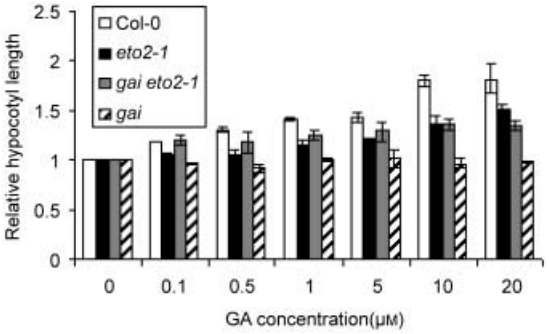

Fig.11 Gibberellin (GA) dose–response curve for hypocotyl length of 8-d-old light-grown Arabidopsis seedlings. Wild-type and mutant seedlings (gibberellin-insensitive (*gai*), ethylene-overproducing 2-1 (*eto2-1*) and *gai eto2-1*) were grown in long-day conditions (16 h light : 8 h dark) on low-nutrient medium supplemented with an increasing concentration of GA_3. Graphs represent relative hypocotyl length; error bars, ± SD.

stress-induced responses, ethylene and GAs also concertedly control germination (Karssen *et al.*, 1989; Ogawa *et al.*, 2003; Chiwocha *et al.*, 2005), cell elongation in hypocotyls (Collett *et al.*, 2000; Saibo *et al.*, 2003) and roots (Achard *et al.*, 2003), formation of stomata (Saibo *et al.*, 2003) and maintenance of the apical hook (Achard *et al.*, 2003; Vriezen *et al.*, 2004). More recently, evidence was found for a role of ethylene in floral transition (Achard *et al.*, 2006, 2007). It was shown that ethylene causes a delay in flowering time in wild-type Arabidopsis and that this effect is almost entirely abolished in a quadruple loss-of-function DELLA mutant (*rga-24 gai-t6 rgl1-1 rgl2-1*) (Achard *et al.*, 2006).

In this study, we have tried to extend our understanding of interactions between the ethylene and GA pathways by analysis of growth and development of the *gai eto2-1* double mutant. Both single mutations lead to negative effects on growth.

Temporal gene expression patterns and protein stability determine the stage of development at which a mutant phenotype will be observed. In wild-type Arabidopsis, *ACS5* (At5g65800) expression is very high at the seedling stage, but drops dramatically after development of the first leaf (Schmid *et al.*, 2005; AtGenExpress: http://web.uni-frankfurt.de/fb15/botanik/mcb/AFGN/atgenex.htm). In the *eto2-1* background, *ACS5* mRNA accumulates to the same levels as in the wild type, but, as a result of an increase in protein stability, ethylene production and responses such as inhibition of cell elongation are enhanced (Vogel *et al.*, 1998). *GAI* (At1g14920) is highly expressed during germination, but at 6 DAG its expression has already decreased (Schmid *et al.*, 2005); moreover, the mRNA levels in *gai* were comparable to those in the wild type, while

protein stability was enhanced (Peng *et al.*, 1997). Because of the repressor character of GAI, increased protein stability leads to a stronger inhibition of GA responses in the mutant. As GAs are responsible for cell elongation, the lack of GA response causes a dwarfed phenotype in the *gai* mutant.

Combined gain-of-function mutations in both *GAI* and *ETO2* resulted in strong phenotypes at all stages of development. Although at the seedling stage (until 8 DAG) the double mutant behaved intermediate between the two single mutants, the growth parameters of roots and shoots of older plants (from day 8 onwards) indicated an additive or even synergistic growth inhibition in *gai eto2-1* (Figs 1, 4). One possible cause for this double-mutant phenotype could be an additional enhancement of ethylene biosynthesis by *GAI*. However, measurements of ethylene emanation showed that, in contrast to *eto2-1*, ethylene biosynthesis was not increased in *gai eto2-1*. This observation implies that a functional GA-response pathway is required for increased ethylene biosynthesis in the *eto2-1* single mutant. It further indicates that the absence of active GA signalling caused by the dominant gain-of-function mutation in *GAI* negatively influences ethylene biosynthesis in the double mutant. The nature of this interaction remains to be investigated, but, as *eto2-1* is affected in the stability of the *ACS5* protein, and *gai* has altered stability in one of the DELLA proteins (Peng *et al.*, 1997; Vogel *et al.*, 1998), it may occur at the protein level, possibly at the 26S proteasome. Our findings support the existence of an additional mode of ACS degradation, which is not mediated by ETO1. Whether or not this pathway is the same as the ETO1-independent cytokinin-inhibited pathway suggested by Chae & Kieber (2005) remains to be investigated. Alternatively, the *gai* mutation could result in lower *ACS5* (*eto2-1*) gene expression in the double mutant. In contrast to ethylene production, the ethylene responsiveness of *gai eto2-1* at low concentrations of ethylene was enhanced in the light as compared with both the wild type and *eto2-1* (Fig. 8). Although differential responsiveness was not found in darkness, double mutants displayed a complete triple response in 4-d-old etiolated seedlings in the absence of ethylene (data not shown). Taking these findings together, it can be concluded that, despite the lower ethylene production, the growth inhibition of the double mutant compared with the *eto2-1* single mutant may – at least in part – be caused by enhanced ethylene responsiveness. However, as the morphological phenotype of the enhanced ethylene response is subtle, a more detailed analysis is required. To that end, the expression of an ethylene-inducible reporter gene (e.g. EBS::GUS; Stepanova *et al.*, 2007) in the presence of different concentrations of ethylene could be compared in the wild type and the single and double mutants at different developmental stages.

The phenotype of the double mutant was either reminiscent of that of one of the parental lines (*eto2-1*-like in lateral root formation (Fig. 3), or *gai*-like in ethylene-emanation (Fig. 7)), additive (in inflorescence length; Supplementary Material Fig. S2) or even synergistic (in shoot surface enlargement; Fig. 4), indicating that the nature of the interaction between ethylene and GA is both spatially and temporally dependent. Ethylene was shown to antagonize the GA response by stabilizing DELLA proteins, RGA in particular (Achard *et al.*, 2003, 2006; Vriezen *et al.*, 2004). However, recent evidence suggests the existence of a DELLA-independent GA pathway. Cao *et al.* (2006) demonstrated that, even in processes known to be controlled in a DELLA-dependent way, such as seed germination and floral development, only half of all GA-response genes are regulated by DELLA proteins. Moreover, within this group of genes, differences were observed related to the developmental process, as a different set of genes was influenced in germination compared with floral development. It can therefore be speculated that stage-dependent forms of ethylene–GA crosstalk may exist, either based on the described interaction at the level of DELLA proteins, or on a DELLA-independent mechanism. To test this hypothesis, it might be interesting to study the expression pattern of both DELLA-dependent and DELLA-independent GA response genes upon GA treatment of ethylene mutants and a combination with multiple DELLA loss-of-function mutants in parallel with wild type or *ga1-3* mutants treated with GA in combination with an ethylene action inhibitor, at several stages of development.

Communication between shoots and roots is a crucial factor determining overall plant architecture. Although *gai eto2-1* had the smallest roots and shoots, the shoot:root ratio was the highest for the double mutant (55 and 75% increase compared with wild-type at 10 and 12 DAG, respectively; Fig. 5), indicating stronger relative growth of the shoot as compared with all other genotypes. The enhanced shoot:root ratio indicates a redirection of the energy of the plant to shoot growth, suppressing root development, as indicated by the decrease in root growth rate from day 8 onwards. As more lateral roots were produced in *gai eto2-1* plants older than 8 d, a loss of primary root dominance was evident. Shoot growth reached a maximum shortly thereafter (between days 10 and 12). Long-distance source-to-sink transport of components such as sucrose and cytokinins has been shown to be important in floral induction. Although there is no direct evidence yet, it is possible that long-distance transport of GA is also important in these processes (Bernier & Périlleux, 2005). Our observation that the ethylene-induced delay in flowering was increased in the double mutant as compared with both single mutants indicates that an interaction between ethylene and GA pathways may be involved in this process, although *gai* remains the major contributor to delay in floral initiation.

Measurements of GA content showed clear differences in *gai eto2-1* as compared with both single mutants, especially for GA_4, which is known to be the most active GA in the vegetative stage of plant development in Arabidopsis (Hooley *et al.*, 1991). It has been reported previously that the GA content in *gai* is higher as a result of a feedback mechanism on GA biosynthesis (Talon *et al.*, 1990; Phillips *et al.*, 1995; Xu *et al.*,

1995; Cowling *et al.*, 1998). The higher GA concentrations in the *gai* single mutant and the double mutant were concomitant with higher expression levels of GA-biosynthesis genes, supporting the feedback hypothesis. The enhanced concentrations of GA_4 in the double mutant corresponded to higher expression of the three *GA20ox* genes examined in combination with higher expression of *GA3ox1*. In the double mutant, the enhanced responsiveness to ethylene could be responsible for further stabilization of DELLA proteins, hyperactivating the feedback mechanism, resulting in higher bioactive GA concentrations. However, this was not reflected in our expression analysis. In particular, the similar levels of *GA3ox1* and *GA20ox* expression in *gai* and *gai eto2-1* appear inconsistent with the strong difference in GA_4 content in these genotypes. However, in Arabidopsis, the GA 3-oxidase family consists of at least four members (Hedden *et al.*, 2002), so other *GA3ox* genes may be responsible for the increased GA_4 concentrations in *gai eto2-1*. Alternatively, another explanation for this discrepancy might be found in a modulation of GA enzyme stability by ethylene. Importantly, not only the concentration of bioactive GA, but also the GA response was enhanced in *gai eto2-1* as compared with the *gai* single mutant. This response may be controlled by a DELLA-independent mechanism, or may suggest that the mutant form of GAI in *gai eto2-1* is subject to an ethylene-driven degradation mechanism, probably by post-translational modification of the mutant GAI protein.

In conclusion, our data indicate that the absence of an active GA-signalling cascade suppresses the higher ethylene biosynthesis seen in *eto2-1* while the responsiveness to ethylene is slightly enhanced. The suppression of ethylene biosynthesis in the double mutant suggests that the absence of active GA signalling may affect the stability of ethylene-biosynthesis enzymes in a negative feedback mechanism. The enhanced sensitivity to GA in the double mutant indicates a reciprocal influence of the two pathways on one another. This is also corroborated by earlier data demonstrating that ACC enhances the activity of the GA-biosynthesis gene *GA1* (Vriezen *et al.*, 2004).

Acknowledgments

This work was supported by grants from the Fund for Scientific Research-Flanders and The Belgian Science Policy Office to DVDS. TM, NH, PH and DVDS gratefully acknowledge funding from the European Union (RTNI-2000-00090-INTEGA).

References

Achard P, Baghour M, Chapple A, Hedden P, Van Der Straeten D, Genschik P, Moritz T, Harberd NP. 2007. The plant stress hormone ethylene controls floral transition via DELLA-dependent regulation of floral meristem-identity genes. *Proceedings of the National Academy of Sciences, USA* **104**: 6484–6489.

Achard P, Cheng H, De Grauwe L, Decat J, Schoutteten H, Moritz T, Van Der Straeten D, Peng J, Harberd NP. 2006. Integration of plant responses to environmentally activated phytohormonal signals. *Science* **311**: 91–94.

Achard P, Vriezen WH, Van Der Straeten D, Harberd NP. 2003. Ethylene regulates *Arabidopsis* development via the modulation of DELLA protein growth repressor function. *Plant Cell* **15**: 2816–2825.

Beemster GT, Baskin TI. 1998. Analysis of cell division and elongation underlying the developmental acceleration of root growth in *Arabidopsis thaliana*. *Plant Physiology* **116**: 1515–1526.

Bernier G, Périlleux C. 2005. A physiological overview of the genetics of flowering control. *Plant Biotechnology Journal* **3**: 3–16.

Cao D, Cheng H, Wu W, Soo HM, Peng J. 2006. Gibberellin mobilizes distinct DELLA-dependent transcriptome to regulate seed germination and floral development in *Arabidopsis*. *Plant Physiology* **142**: 509–525.

Chae HS, Kieber JJ. 2005. *Eto Brute*? Role of ACS turnover in regulating ethylene biosynthesis. *Trends in Plant Science* **10**: 291–296.

Chaerle L, Hagenbeek D, De Bruyne E, Valcke R, Van Der Straeten D. 2004. Thermal and chlorophyll-fluorescence imaging distinguish plant–pathogen interactions at an early stage. *Plant and Cell Physiology* **45**: 887–896.

Chiwocha SD, Cutler AJ, Abrams SR, Ambrose SJ, Yang J, Ross AR, Kermode AR. 2005. The *etr1-2* mutation in *Arabidopsis thaliana* affects the abscisic acid, auxin, cytokinin and gibberellin metabolic pathways during maintenance of seed dormancy, moist-chilling and germination. *Plant Journal* **42**: 35–48.

Collett CE, Harberd NP, Leyser O. 2000. Hormonal interactions in the control of *Arabidopsis* hypocotyl elongation. *Plant Physiology* **124**: 553–562.

Cowling RJ, Kamiya Y, Seto H, Harberd NP. 1998. Gibberellin dose–response regulation of *GA4* gene transcript levels in *Arabidopsis*. *Plant Physiology* **117**: 1195–1203.

De Grauwe L, Vriezen WH, Bertrand S, Phillips A, Vidal AM, Hedden P, Van Der Straeten D. 2007. Reciprocal influence of ethylene and gibberellins on response-gene expression in *Arabidopsis thaliana*. *Planta* **226**: 485–498.

Dill A, Sun T-P. 2001. Synergistic derepression of gibberellin signalling by removing RGA and GAI function in *Arabidopsis thaliana*. *Genetics* **159**: 777–785.

Dill A, Thomas SG, Hu J, Steber CM, Sun T-P. 2004. The *Arabidopsis* F-box protein SLEEPY1 targets gibberellin signalling repressors for gibberellin-induced degradation. *Plant Cell* **16**: 1392–1405.

Fu X, Harberd NP. 2003. Auxin promotes *Arabidopsis* root by modulating gibberellin response. *Nature* **421**: 740–743.

Fu X, Richards DE, Ait-Ali T, Hynes LW, Ougham H, Peng J, Harberd NP. 2002. Gibberellin-mediated proteasome-dependent degradation of the barley DELLA protein SLN1 repressor. *Plant Cell* **14**: 3191–3200.

Fu X, Richards DE, Fleck B, Xie D, Burton N, Harberd NP. 2004. The *Arabidopsis* mutant sly1^{gar2-1} protein promotes plant growth by increasing the affinity of the SCF^{SLY1} E3 ubiquitin ligase for DELLA protein substrates. *Plant Cell* **16**: 1406–1418.

Griffiths J, Murase K, Rieu I, Zentella R, Zhang ZL, Powers SJ, Gong F, Phillips AL, Hedden P, Sun T-P *et al.* 2006. Genetic characterization and functional analysis of the GID1 gibberellin receptors in *Arabidopsis*. *Plant Cell* **18**: 3399–3414.

Hedden P, Phillips AL, Rojas MC, Carrera E, Tudzynski B. 2002. Gibberellin biosynthesis in plants and fungi: a case of convergent evolution? *Journal of Plant Growth Regulation* **20**: 319–331.

Hooley R, Beale MH, Smith SJ. 1991. Gibberellin perception at the plasma membrane of *Avena fatua* aleurone protoplasts. *Planta* **183**: 274–280.

Karssen C, Zagorski S, Kepczynski J, Groot S. 1989. Key role for endogenous gibberellins in the control of seed germination. *Annals of Botany* **63**: 71–80.

Kende H, van der Knaap E, Cho HT. 1998. Deepwater rice: a model plant to study stem elongation. *Plant Physiology* **118**: 1105–1110.

Kieber JJ, Rothenberg M, Roman G, Feldmann KA, Ecker JR. 1993. CTR1,

a negative regulator of the ethylene response pathway in *Arabidopsis*, encodes a member of the Raf family of protein kinases. *Cell* **72**: 427–441.

Lee S, Cheng H, King KE, Wang W, He Y, Hussain A, Lo J, Harberd NP, Peng J. 2002. Gibberellin regulates *Arabidopsis* seed germination via RGL2, a GAI/RGA-like gene whose expression is up-regulated following imbibition. *Genes and Development* **16**: 646–658.

McGinnis K, Thomas S, Soule J, Strader L, Zale J, Sun T-P, Steber C. 2003. The *Arabidopsis SLEEPY1* gene encodes a putative F-box subunit of an SCF E3 ubiquitin ligase. *Plant Cell* **15**: 1120–1130.

Moritz T, Olsen JE. 1995. Comparison between high-resolution selected-ion monitoring, selected reaction monitoring and 4-sector tandem mass-spectometry in quantitative-analysis of gibberellins in milligram amants of plant-tissue. *Analytical Chemistry* **67**: 1711–1716.

Nakajima M, Shimada A, Takashi Y, Kim YC, Park SH, Ueguchi-Tanaka M, Suzuki H, Katoh E, Iuchi S, Kobayashi M *et al.* 2006. Identification and characterization of *Arabidopsis* gibberellin receptors. *Plant Journal* **46**: 880–889.

Narang RA, Bruene A, Altmann T. 2000. Analysis of phosphate acquisition efficiency in different *Arabidopsis* accessions. *Plant Physiology* **124**: 1786–1799.

Ogawa M, Hanada A, Yamauchi Y, Kuwahara A, Kamiya Y, Yamaguchi S. 2003. Gibberellin biosynthesis and response during *Arabidopsis* seed germination. *Plant Cell* **15**: 1591–1604.

Peng J, Carol P, Richards DE, King KE, Cowling RJ, Murphy GP, Harberd NP. 1997. The *Arabidopsis GAI* gene defines a signalling pathway that negatively regulates gibberellin responses. *Genes and Development* **11**: 3194–3205.

Phillips AL, Ward DA, Uknes S, Appleford NEJ, Lange T, Huttly AK, Gaskin P, Graebe JE, Hedden P. 1995. Isolation and expression of three gibberellin 2-oxidase cDNA clones from *Arabidopsis*. *Plant Physiology* **108**: 1049–1057.

Ramakers C, Ruijter JM, Deprez RH, Moorman AF. 2003. Assumption-free analysis of quantitative real-time polymerase chain reaction (PCR) data. *Neuroscience Letters* **339**: 62–66.

Richards DE, King LE, Ait-Ali T, Harberd NP. 2001. How gibberellin regulates plant growth and development: a molecular genetic analysis of gibberellin signalling. *Annual Review of Plant Physiology and Plant Molecular Biology* **52**: 67–88.

Rodrigues-Pousada RA, De Rycke R, Dedonder A, Van Caeneghem W, Engler G, Van Montagu M, Van Der Straeten D. 1993. The *Arabidopsis* 1-aminocyclopropane-1-carboxylate synthase gene 1 is expressed during early development. *Plant Cell* **5**: 897–911.

Saibo NJM, Vriezen WH, Beemster G, Van Der Straeten D. 2003. Growth and stomata development of Arabidopsis hypocotyls are controlled by gibberellins and modulated by ethylene and auxins. *Plant Journal* **33**: 989–1000.

Schmid M, Davison TS, Henz SR, Pape UJ, Demar M, Vingron M, Scholkopf B, Weigel D, Lohmann JU. 2005. A gene expression map of *Arabidopsis thaliana* development. *Nature Genetics* **37**: 501–506.

Silverstone AL, Ciampaglio CN, Sun T-P. 1998. The *Arabidopsis RGA* gene encodes a transcriptional regulator repressing the gibberellin signal transduction pathway. *Plant Cell* **10**: 155–169.

Silverstone AL, Jung HS, Dill A, Kawaide H, Kamiya Y, Sun T-P. 2001. Repressing a repressor: Gibberellin-induced rapid destruction of the RGA protein in *Arabidopsis*. *Plant Cell* **13**: 1555–1566.

Smalle J, Haegman M, Kurepa J, Van Montagu M, Van Der Straeten D. 1997. Ethylene can stimulate *Arabidopsis* hypocotyl elongation in the light. *Proceedings of the National Academy of Sciences, USA* **94**: 2756–2761.

Stepanova AN, Yun J, Likhacheva AV, Alonso JM. 2007. Multilevel interactions between ethylene and auxin in *Arabidopsis* roots. *Plant Cell* **19**: 2169–2185.

Sun T-P, Goodman HM, Ausubel FM. 1992. Cloning the *Arabidopsis GA1* locus by genomic subtraction. *Plant Cell* **4**: 119–128.

Talon M, Koornneef M, Zeevaart JAD. 1990. Accumulation of C19-gibberellins in the gibberellin-insensitive dwarf mutant *gai* of *Arabidopsis thaliana* (L.) Heynh. *Planta* **182**: 501–505.

Vandenbussche F, Van Der Straeten D. 2004. Shaping the shoot: a circuitry that integrates multiple signals. *Trends in Plant Science* **9**: 499–506.

Vogel JP, Woeste KE, Theologis A, Kieber JJ. 1998. Recessive and dominant mutations in the ethylene biosynthetic gene *ACS5* of *Arabidopsis* confer cytokinin insensitivity and ethylene overproduction, respectively. *Proceedings of the National Academy of Sciences, USA* **95**: 4766–4771.

Vriezen WH, Achard P, Harberd N, Van Der Straeten D. 2004. Ethylene-mediated enhancement of apical hook formation in etiolated *Arabidopsis thaliana* seedlings is gibberellin dependent. *Plant Journal* **37**: 505–516.

Vriezen WH, Zhou Z, Van Der Straeten D. 2003. Regulations of submergence-induced enhanced shoot elongation in *Oryza sativa* L. *Annals of Botany* **91**: 263–270.

van der Weele CM, Jiang HS, Palaniappan KK, Ivanov VB, Palaniappan K, Baskin TI. 2003. A new algorithm for computational image analysis of deformable motion at high spatial and temporal resolution applied to root growth. Roughly uniform elongation in the meristem and also, after an abrupt acceleration, in the elongation zone. *Plant Physiology* **132**: 1138–1148.

Wen CK, Chang C. 2002. *Arabidopsis RGL1* encodes a negative regulator of gibberellin responses. *Plant Cell* **14**: 87–100.

Xu Y-L, Li L, Wu K, Peeters AJM, Gage DA, Zeevaart JAD. 1995. The *GA5* locus of *Arabidopsis thaliana* encodes a multifunctional gibberellin 20-oxidase: Molecular cloning and functional expression. *Proceedings of the National Academy of Sciences, USA* **92**: 6640–6644.

Supplementary Material

The following supplementary material is available for this article online:

Fig. S1 Ethylene emanation from bolting plants (plants forming a bolting stem of ± 1 cm): Columbia (Col-0) (16 d), ethylene-overproducing 2-1 (*eto2-1*) (18 d), gibberellin-insensitive (*gai*) *eto2-1* (22 d) and *gai* (22 d).

Fig. S2 Measurements of the total inflorescence length of mature plants.

Fig. S3 Gibberellin (GA) concentrations in rosettes of Columbia (Col-0), ethylene-overproducing 2-1 (*eto2-1*), gibberellin-insensitive (*gai*) *eto2-1* and *gai*.

Table S1 Primer sequences as used for real-time PCR

This material is available as part of the online article from http://www.blackwell-synergy.com/doi/abs/10.1111/j.1469-8137.02263.x
(This link will take you to the article abstract.)

Please note: Blackwell Publishing are not responsible for the content or functionality of any supplementary materials supplied by the authors. Any queries (other than about missing material) should be directed to the *New Phytologist* Central Office.